Robotica (2004) volume 22, pp. 41–50. © 2004 Cambridge University Press
DOI: 10.1017/S0263574703005393 Printed in the United Kingdom

Dynamic simulation and experiments for the design of a new 7-dofs biped walking leg module

Giuseppe Carbone,* Yu Ogura,† Hun-ok Lim‡§ Atsuo Takanishi†§ and Marco Ceccarelli*

(Received in Final Form: May 29, 2003)

SUMMARY
In this paper the mechanical design for a new 7-dofs leg is investigated as a walking module for a humanoid robot. In particular, a dynamic simulation is deduced by means of a Newton-Euler formulation and implemented numerically in order to compute the needed input actuator torques. A simulation is carried out for a similar built leg prototype that is used as a walking module for WABIAN-RIV (WAseda BIped humANoid robot-Revised IV). Experimental tests are carried out on this existing leg in order to validate the proposed formulation for a similar application. Thus, the validated formulation has been used in order to design the actuators for a new leg prototype.

KEYWORDS: Walking module; Dynamic simulation; Humanoid robot.

* Laboratory of Robotics and Mechatronics, DiMSAT – University of Cassino, Via Di Biasio 43-03043 Cassino (Fr) (Italy).
E-mail: carbone/ceccarelli@ing.unicas.it
† Graduate School of Science and Engineering, Waseda University, 3-4-1 Ookubo, Shinjuku-ku, Tokyo 169–8555 (Japan).
E-mail: 601q023@mn.waseda.ac.jp
‡ Kanagawa Institute of Technology, Department of System Design Engineering, 1030 Shimoogino, Atugi, Kanagawa 243-0292 (Japan).
E-mail: holim@sd.kanagawa-it.ac.jp
§ Humanoid Robotics Institute, Waseda University, 3-4-1 Ookubo, Shinjuku-ku, Tokyo 169–8555 (Japan).
E-mail: takanisi@waseda.jp

1. INTRODUCTION

The development of robots that are able to imitate the human movements is one of the most fascinating activities of the researchers in the field of robotics. Humanoid robots are complex mechatronic systems consisting of a high number of integrated components requiring developments in many different fields.[1–4]

One of the main components of a humanoid robot is the leg module that has been studied by many researchers as, for example, in references [5–17]. Waseda University, which is one of the leading Institutions in the specific field, has developed many biped robots prototypes that have been named as WL series (Waseda Leg). Some examples are shown in Figure 1. In particular, Figure 1a shows the WL-1 prototype, which was built on the basis of a human leg mechanism in 1967; Figure 2b shows the WL-10R, which achieved forward and backward walking, turning on plane in 1983; Figure 3b shows the WL-12, which was built to realize more human-like motion in 1986.[18–20]

In this paper, a mechanical design activity is reported for the development of a new prototype of a leg to be used as walking module in a new humanoid robot. This new humanoid prototype, which Takanishi et al. have been developing at Waseda University, is supposed to have an anthropomorphic design of a size of a human child and, in particular, an overall weight of about 500 N and a maximum height of about 1.2 m.

The dynamic effects during the biped walking and significant contribution of the actuators to the overall performances have been pointed out, for example, in

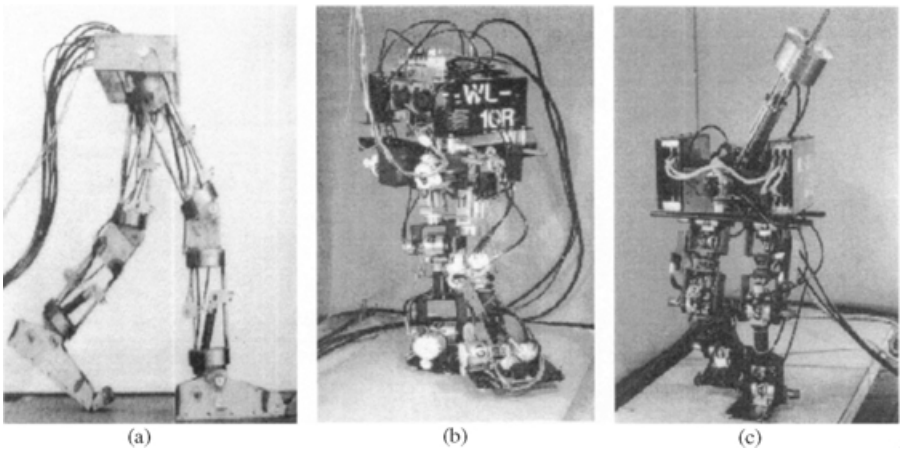


Fig. 1. Prototypes of walking modules that have been developed at Waseda University[18–20]: (a) WL-1; (b) WL-10R; (c) WL-12.

https://doi.org/10.1017/S0263574703005393 Published online by Cambridge University Press

references [13–17]. Therefore, in this paper, a dynamic simulation by means of a Newton-Euler formulation is carried out in a Matlab environment in order to properly design the needed actuators.

2. A KINEMATIC MODEL FOR THE A PROTOTYPE

The new leg prototype is supposed to have a kinematic model similar to that of the leg module of the WABIAN-RIV humanoid robot,[18–20] but with one more degree of freedom. Figures 2 and 3 show detailed kinematic models for the leg module of the WABIAN-RIV and for the new prototype, respectively.

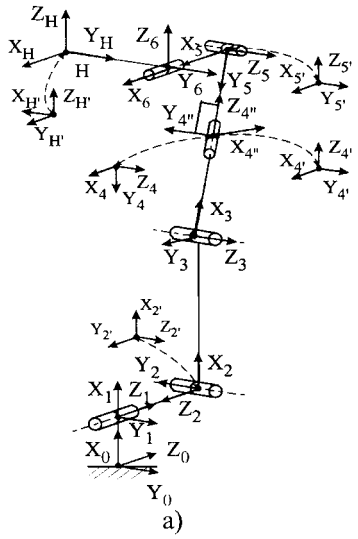
It is worth noting that in these models the Denavit-Hartenberg (D-H) convention shown in Figure 4 has been used in order to define the position and orientation of the link coordinate frames $X_iY_iZ_i$. The Denavit-Hartenberg link parameters are: a_{i-1}, which is the distance from Z_{i-1} to Z_i axes as measured along X_{i-1} axis; d_i, which is the distance from X_{i-1} to X_i axes as measured along Z_i axis; α_i, which is the angle between Z_{i-1} and Z_i axes as measured about X_{i-1} axis; θ_i, which is the angle between X_{i-1} and X_i axes as measured about Z_{i-1} axis. The angles are assumed positive, counterclockwise about the rotation axis.

By using the above-mentioned parameters, the transformation matrix $\mathbf{T}_i^{i-1}$ that expresses the relation between frame i and i − 1 can be written as:

$$\mathbf{T}_i^{i-1} = \begin{bmatrix} c\theta_i & -s\theta & 0 & a_{i-1} \\ s\theta_1\, c\alpha_{i-1} & c\theta_i\, c\alpha_{i-1} & -s\alpha_{i-1} & -d_1\, s\alpha_{i-1} \\ s\theta_i\, s\alpha_{i-1} & c\theta_i\, s\alpha_{i-1} & c\alpha_{i-1} & d_i\, c\alpha_{i-1} \\ 0 & 0 & 0 & 1 \end{bmatrix} \quad (1)$$

where $c\alpha_i$, $s\alpha_i$, $c\theta_i$ and $s\theta_i$ are shorthands of $\cos\alpha_i$, $\sin\alpha_i$, $\cos\theta_i$ and $\sin\theta_i$, respectively. In addition, a rotation matrix $\mathbf{R}_i^{i-1}$ can be computed from Equation (1) by extracting the first three rows and columns.

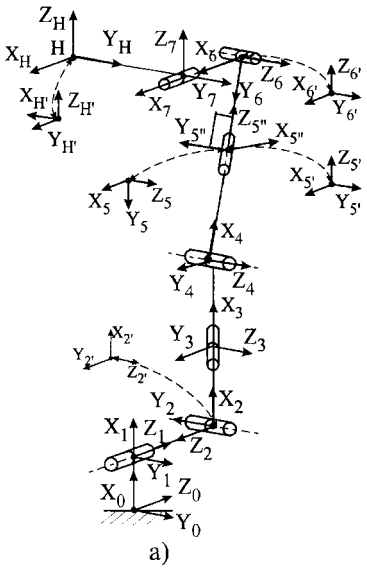
By considering the references frames of Figures 2a and 3a, the D-H link parameters for the kinematic chains of the leg module of WABIAN-RIV and new leg prototype can be determined, as shown in Figures 2b and 3b, respectively.



D-H par. / Link No.	$\alpha_{(i-1)}$ [deg]	$a_{(i-1)}$ [mm]	d_i [mm]	θ_i [deg]
1	0	a_0=185	0	θ_1
2	180	0	-d_2=0	0
2'	90	0	0	θ_2
3	0	a_2=300	0	θ_3
4	0	a_3=223.5	0	90
4'	90	0	0	0
4''	0	0	0	θ_4+180
5	90	0	-d_5=130	180
5'	90	0	0	θ_5
6	θ_6	a_5=0	0	0
H'	0	0	d_6=0	-90
H	0	0	0	90

b)

Fig. 2. Leg module of WABIAN-RIV: (a) a Kinematic scheme; (b) its D-H parameters.



D-H par. / Link No.	$\alpha_{(i-1)}$ [deg]	$a_{(i-1)}$ [mm]	d_i [mm]	θ_i [deg]
1	0	a_0=65	0	θ_1
2	180	0	-d_2=0	0
2'	90	0	0	θ_2
3	θ_3	a_2=260	0	0
4	0	a_3=140	0	θ_4
5	0	a_4	0	90
5'	90	0	0	0
5''	90	0	0	θ_5+180
6	90	0	-d_5=120	180
6'	θ_6	a_5=0	0	0
7	0	0	d_6=0	-90
H'	0	0	d_7=0	-90
H	0	0	0	90

b)

Fig. 3. New 7-dofs leg module: (a) a Kinematic scheme; (b) its D-H parameters.

https://doi.org/10.1017/S0263574703005393 Published online by Cambridge University Press

By using Equation (1) and the D-H link parameters in Figures 2b and 3b, the transformation matrices expressing the relation between the frames in Figures 2a and 3a can be straightforward derived for the leg module of the WABIAN-RIV and new leg prototype, respectively.

3. NEWTON-EULER DYNAMICS FORMULATION

A dynamics analysis can be carried out in order to design the actuators for a leg prototype. In particular, the torques that are needed in order to perform a given trajectory of the leg can be computed by using a suitable Newton-Euler dynamics formulation. It is worth noting that this formulation is effective even for a more complex system as pointed out for example in reference [21]. An iterative algorithm can be derived, as proposed in reference [22]. It is composed of outward and inward iterations. The outward iterations can be written by considering $i=0,1,\ldots,n-1$ in the form:

$$
\begin{aligned}
&{}^{i+1}\boldsymbol{\omega}_{i+1} = {}^{i+1}_{i}\mathbf{R}\,{}^{i}\boldsymbol{\omega}_{i} + \dot{\boldsymbol{\theta}}_{i+1}\,{}^{i+1}\hat{\mathbf{Z}}_{i+1}\\
&{}^{i+1}\dot{\boldsymbol{\omega}}_{i+1} = {}^{i+1}_{i}\mathbf{R}\,{}^{i}\dot{\boldsymbol{\omega}}_{i} + {}^{i+1}_{i}\mathbf{R}\,{}^{i}\boldsymbol{\omega}_{i}\times\dot{\boldsymbol{\theta}}_{i+1}\,{}^{i+1}\hat{\mathbf{Z}}_{i+1} + \ddot{\boldsymbol{\theta}}_{i+1}\,{}^{i+1}\hat{\mathbf{Z}}_{i+1}\\
&{}^{i+1}\dot{\mathbf{v}}_{i+1} = {}^{i+1}_{i}\mathbf{R}\left({}^{i}\boldsymbol{\omega}_{i}\times{}^{i}\mathbf{P}_{i+1} + {}^{i}\boldsymbol{\omega}_{i}\times({}^{i}\boldsymbol{\omega}_{i}\times{}^{i}\mathbf{P}_{i+1}) + {}^{i}\dot{\mathbf{v}}_{i}\right)\\
&{}^{i+1}\dot{\mathbf{v}}_{Ci+1} = {}^{i+1}\boldsymbol{\omega}_{i+1}\times{}^{i+1}\mathbf{P}_{Ci+1} + {}^{i+1}\boldsymbol{\omega}_{i+1}\times\\
&\qquad\left({}^{i+1}\boldsymbol{\omega}_{i+1}\times{}^{i+1}\mathbf{P}_{Ci+1}\right) + {}^{i+1}\dot{\mathbf{v}}_{i+1}\\
&{}^{i+1}\mathbf{F}_{i+1} = m_{i+1}\,{}^{i+1}\dot{\mathbf{v}}_{Ci+1}\\
&{}^{i+1}\mathbf{N}_{i+1} = {}^{C(i+1)}\mathbf{I}_{i+1}\,{}^{i+1}\dot{\boldsymbol{\omega}}_{i+1} + {}^{i+1}\boldsymbol{\omega}_{i+1}\times{}^{C(i+1)}\mathbf{I}_{i+1}\,{}^{i+1}\boldsymbol{\omega}_{i+1}
\end{aligned}
\tag{2}
$$

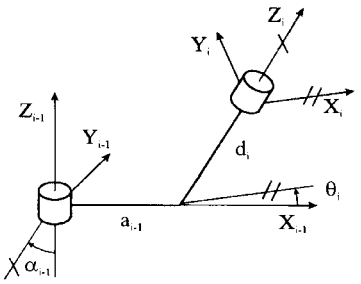


Fig. 4. A scheme for Denavit-Hartenberg parameters.

where n is the number of links; the dot stands for the time derivative operator; x stands for a cross product operator; ${}^{i+1}\omega_{i+1}$ is the angular velocity of the link $i+1$ expressed in the frame $i+1$; ${}^{i+1}_{i}\mathbf{R}$ is the rotation matrix describing the reference frame i in the reference frame $i+1$; θ_{i+1} is the input angle for the joint $i+1$; ${}^{i}\mathbf{P}_{i+1}$ is the vector of the origin of the reference frame $i+1$ in the reference frame i; ${}^{i}\mathbf{P}_{Ci+1}$ is the vector expressing the location of the center of mass $Ci+1$ in the reference frame i; ${}^{i+1}\mathbf{v}_{i+1}$ is the linear velocity of the reference frame $i+1$ as expressed in the $i+1$ reference frame; ${}^{i+1}\mathbf{F}_{i+1}$ and ${}^{i+1}\mathbf{N}_{i+1}$ are the inertial force and torque acting at the center of mass of $i+1$ link as expressed in the $i+1$ link, respectively; m_{i+1} is the mass of the body $i+1$; ${}^{C(i+1)}\mathbf{I}_{i+1}$ is the inertia tensor of the body $i+1$ as written in a frame whose origin is located at center of mass $C_{(i+1)}$.

The inward iterations can be written by considering $i=n,n-1,\ldots,1$ in the form:

$$
\begin{aligned}
&{}^{i}\mathbf{f}_{i} = {}^{i}_{i+1}\mathbf{R}\,{}^{i+1}\mathbf{f}_{i+1} + {}^{i}\mathbf{F}_{i}\\
&{}^{i}\mathbf{n}_{i} = {}^{i}\mathbf{N}_{i} + {}^{i}_{i+1}\mathbf{R}\,{}^{i+1}\mathbf{n}_{i+1} + {}^{i}\mathbf{P}_{Ci}\times{}^{i}\mathbf{F}_{i} + {}^{i}\mathbf{P}_{i+1}\times{}^{i}_{i+1}\mathbf{R}\,{}^{i+1}\mathbf{f}_{i+1}\\
&\boldsymbol{\tau}_{i} = {}^{i}\mathbf{n}_{i}^{T}\hat{\mathbf{Z}}_{i}
\end{aligned}
$$

where $\mathbf{f}_i$ is the force that is exerted on the link i by the link $i-1$; $\mathbf{n}_i$ is the torque that is exerted on the link i by the link $i-1$; τ_i is the actuating torques that is required in the active joints.

It is worth noting that effect of gravity can be considered by setting the acceleration of the base frame as:

$${}^{0}\dot{v}_{0x} = g = 9.81\ \frac{m}{s_2} \tag{4}$$

Forces and torques acting on the leg are shown in the models of Figures 5a and b for the leg module of the WABIAN-RIV and for the new leg prototype, respectively. For example, in Figure 5 $\mathbf{F}_1$, $\mathbf{N}_1$, and $\mathbf{f}_1$, $\mathbf{n}_1$ stand for the inertial force and torque given by the mass and inertia of the link 1 lumped in C_1 and for the force and torque exerted by link 1 on link 0, respectively.

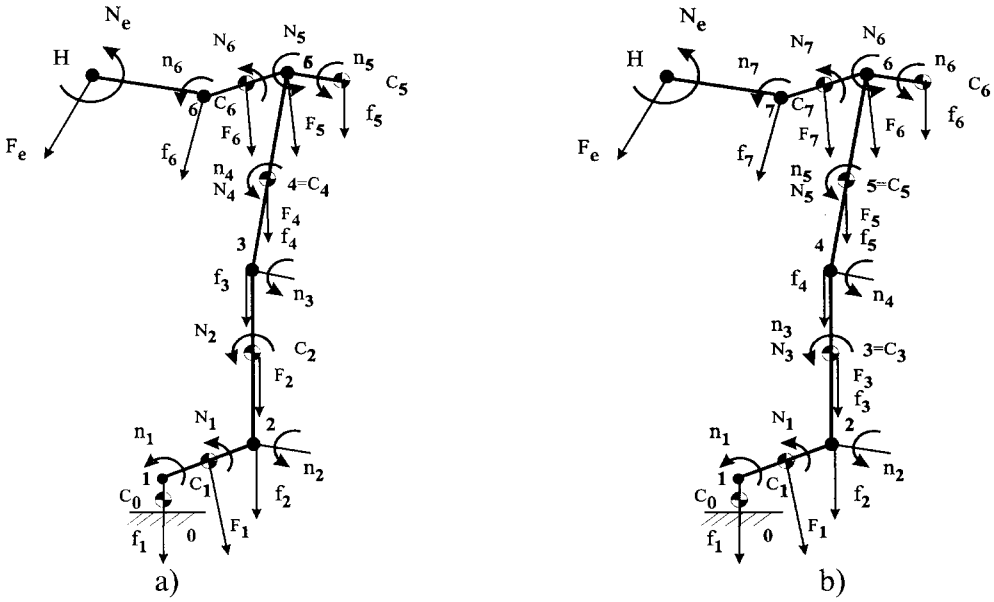


Fig. 5. A model for the forces acting on a leg: (a) WABIAN-RIV design; (b) new leg prototype.

https://doi.org/10.1017/S0263574703005393 Published online by Cambridge University Press

4. A NUMERICAL EVALUATION OF INPUT TORQUES

The above-mentioned formulation can be used in order to carry out a numerical evaluation of the torques that are needed to perform a given movement of a leg. However, it is worth noting that this is an approximated method since friction in the joints and continuous mass distribution have been neglected, although their effect can be limited to a suitable negligible value through suitable design. Therefore, a first numerical evaluation of the needed torques has been carried out on the built leg module of the WABIAN-RIV that is shown in Figure 6.

4.1 input Torques for the Leg Module of WABIAN-RIV

The proposed formulation needs as inputs the kinematics and trajectory of the leg (position, velocity and acceleration of all the joints), mass and inertia distribution. The kinematics for the leg module of a WABIAN-RIV can be given through Equation (1). The D-H parameters can be assumed as reported in Figure 2b. The mass and inertia parameters can be assumed as reported in Table I. It is worth noting that these parameters can be considered as lumped in the joints and center of masses of the leg module of the WABIAN-RIV, defined in Figure 5a.

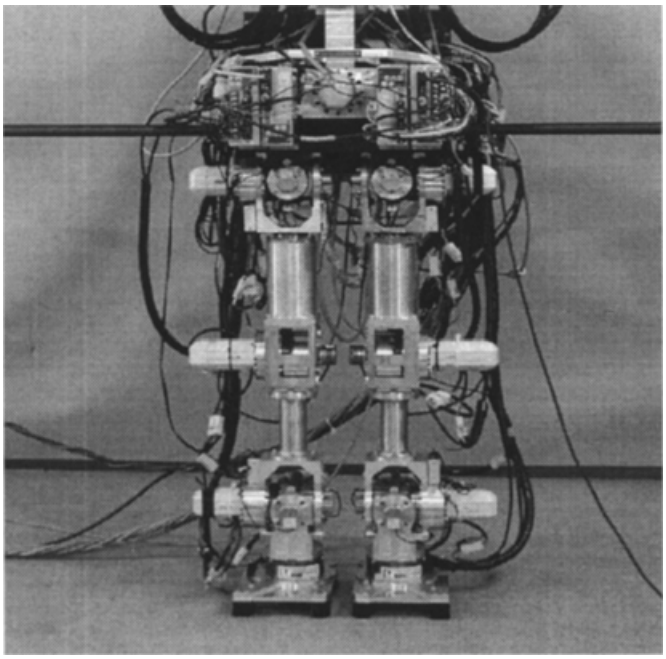


Fig. 6. A built leg module for WABIAN-RIV at Waseda University.

As regards the trajectory, a real motion of the built prototype of the leg module of the WABIAN-RIV can be considered. In fact, during walking each joint of a WABIAN-RIV leg moves according to a joint angle versus time data file generated by a suitable pattern planning algorithm that has been developed in $C++$ environment for experimental tests, as explained in references [23,24]. Therefore, the pattern planning algorithm can be used in order to obtain all the input angles versus time in a suitable format that is needed for simulation purposes. Figure 7 shows a plot of input joint angles versus time for the case of a four steps forward motion at a velocity of 0.2 m/s. The above-mentioned input data have been used for the evaluation of the needed torques by implementing Equations (2)–(4) in a Matlab environment. Results of the proposed numerical dynamics simulation are shown in the plots of the input torques τ_1, τ_2, τ_3, τ_4, τ_5, τ_6 as a function of time in Figure 8.

It is worth noting that the dynamics simulation has been carried out by modelling one leg only. This is because, due to the symmetric design of the WABIAN-RIV, the other leg can be considered to exhibit the same behavior. Moreover, in the model it has been assumed that the simulated leg is always in contact with the floor, while the other leg is in an up-position performing the forward free motion of the leg. This assumption has been chosen since the leg in contact with the ground refers to the most critical case for a leg. However, this is only valid for some input angles. Therefore, in Figure 8 the value of the torques has been set equal to zero in the phases of walking where the chosen model is not valid. It is also worth noting that in the numerical simulation the robot is walking for 9 sec from 10.5 sec to 19.5 sec, as shown in the plot of Figure 7. From 0 to 10.5 sec and from 19.5 sec to 30 sec the robot stands in a static configuration that has been measured by sensors as shown in the plots of Figure 9 and through the dotted lines in the plots of Figure 10. However, the numerical simulation refers only to the dynamic phase of the walking. Thus, the proposed numerical simulation of the dynamic behaviour has been performed only in the range of time from 19.5 sec to 30 sec, as shown in the plots of Figures 8 and 10. Consequently, the plots with continuous lines in Figure 10 are drawn only for the dynamic phase of the walking.

An experimental test has been also carried out for the same case of the numerical simulation and results are shown in Figure 9. The WABIAR R-IV has been moved along the trajectory defined through the joint angles shown in Figure 7. Since the WABIAN-RIV prototype is equipped with torque sensors on each joint of leg module, during the

Table I. Mass and inertia parameters for the built leg module of WABIAN-RIV referring to the model of Figure 5a.

Lumped Mass at the Joint [N]		Lumped Mass at center of mass [N]		Lumped Inertia at center of mass [N m_2]	
m_1	44.75	m_{C1}	0	I_{C1}	0.383
m_2	0	m_{C2}	46.60	I_{C2}	0
m_3	55.94	m_{C3}	3.46	I_{C3}	1.259
m_4	18.70	m_{C4}	0	I_{C4}	0.234
m_5	27.30	m_{C5}	27.60	I_{C5}	0.115
m_6	34.89	m_{C6}	0	I_{C6}	0.119

https://doi.org/10.1017/S0263574703005393 Published online by Cambridge University Press

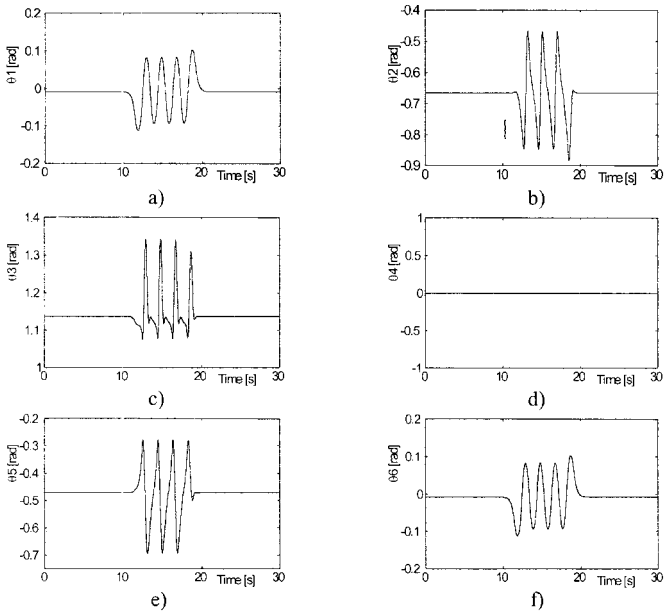


Fig. 7. Joint angles [rad] versus time [sec] as generated by the pattern planning algorithm for a four step forward motion of WABIAN-RIV: (a) θ_1; (b) θ_2; (c) θ_3; (d) θ_4; (e) θ_5; (f) θ_6.

experiment it has been possible to measure the real torques in each joint as function of time. Figures 9a–f show the plots of the input torques τ_1, τ_2, τ_3, τ_4, τ_5, τ_6 as a function of time, respectively, during a real motion. The numerical and experimental results of Figures 8 and 9 have been also reported in Figure 10 in order to compare graphically numerical and experimental results. This comparison shows a good match between numerical and experimental results, both in maximum values and shapes of torque plots versus time. In particular, the maximum absolute difference can be evaluated as 18.5 Nm, and the maximum percentage difference is 9.8%, as also reported in Table II.

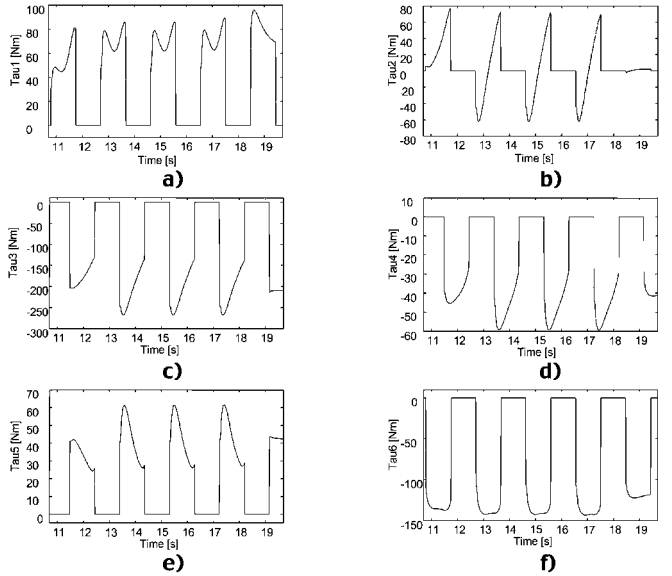


Fig. 8. Input torques [Nm] versus time [sec] as obtained from the numerical dynamics simulation of the leg motion by using the joint angle data in Figure 7: (a) τ_1; (b) τ_2; (c) τ_3; (d) τ_4; (e) τ_5; (f) τ_6.

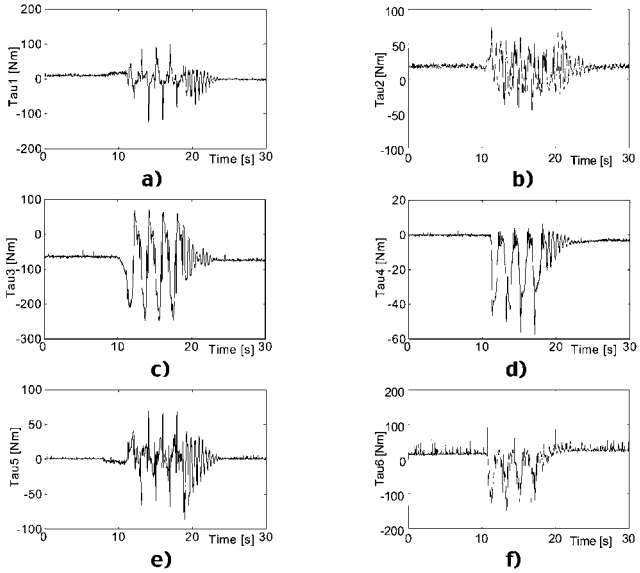


Fig. 9. Input torques [Nm] versus time [sec] as measured experimentally for the leg motion by using the joint angles data in Figure 7: (a) τ_1; (b) τ_2; (c) τ_3; (d) τ_4; (e) τ_5; (f) τ_6.

Numerical dynamics simulations and experimental tests have been carried out also for a four steps right side motion and for a four steps left turning motion, whose plots of input joint angles versus time generated by the pattern planning algorithm are reported in Figures 11 and 12, respectively. Results of the proposed numerical simulation are shown in the plots of the input torques τ_1, τ_2, τ_3, τ_4, τ_5, τ_6 as a function of time in Figures 13 and 14 for a four steps right side motion and for a four steps left turning motion, respectively. Experimental tests have been carried out and the plots of the input torques τ_1, τ_2, τ_3, τ_4, τ_5, τ_6 are the obtained results as

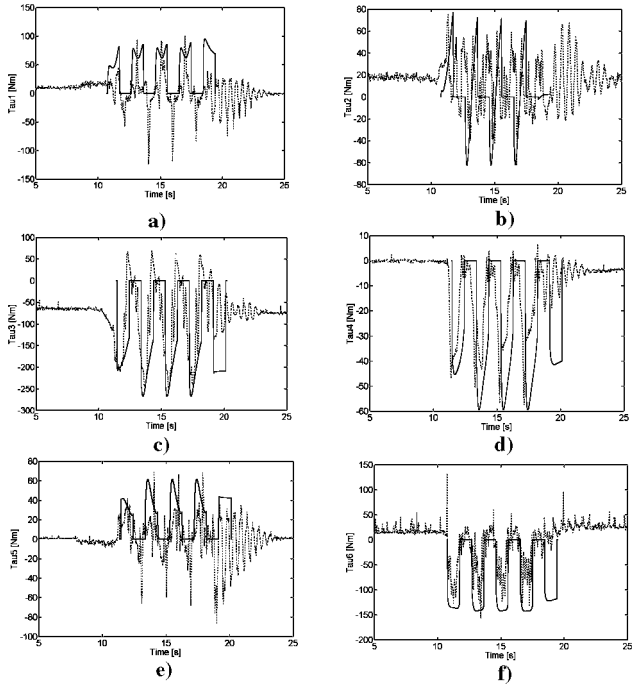


Fig. 10. Comparison of numerically computed (continue line) and experimentally measured (dotted line) input torques [Nm] versus time [sec] the leg motion by using the joint angles data in Figure 7: (a) τ_1; (b) τ_2; (c) τ_3; (d) τ_4; (e) τ_5; (f) τ_6.

https://doi.org/10.1017/S0263574703005393 Published online by Cambridge University Press

Table II. Comparison of the maximum torques obtained from the numerical and experimental data reported in the plots of Figures 8 and 9, respectively.

	τ_{1max}[Nm]	τ_{2max}[Nm]	τ_{3max}[Nm]	τ_{4max}[Nm]	τ_{5max}[Nm]	τ_{6max}[Nm]
Numerical	96.0	− 62.4	− 267.9	− 59.5	61.7	− 143.2
Experimental	100.6	− 61.8	− 249.4	− 57.4	68.4	− 156.6
Absolute difference	− 4.6	0.6	18.5	2.1	− 6.7	− 13.4
Percentage difference	− 4.6%	1.0%	6.9%	3.7%	− 9.8%	− 8.6%

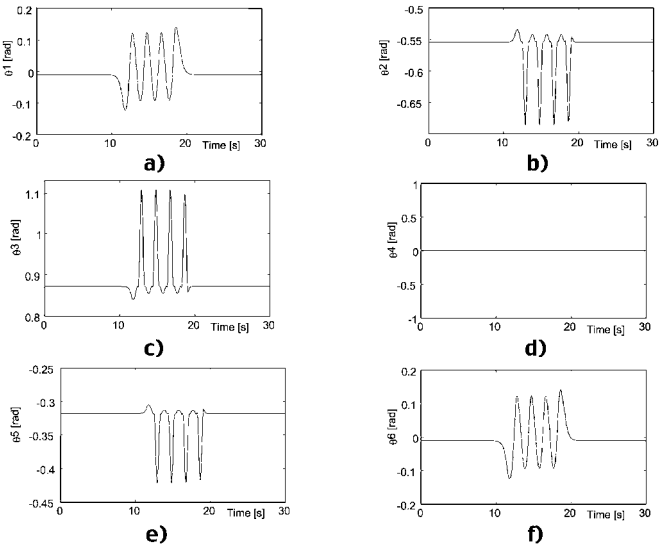


Fig. 11. Joint angles [rad] versus time [sec] generated by the pattern planning algorithm for a four step right side motion of WABIAN-RIV: (a) θ_1; (b) θ_2; (c) θ_3; (d) θ_4; (e) θ_5; (f) θ_6.

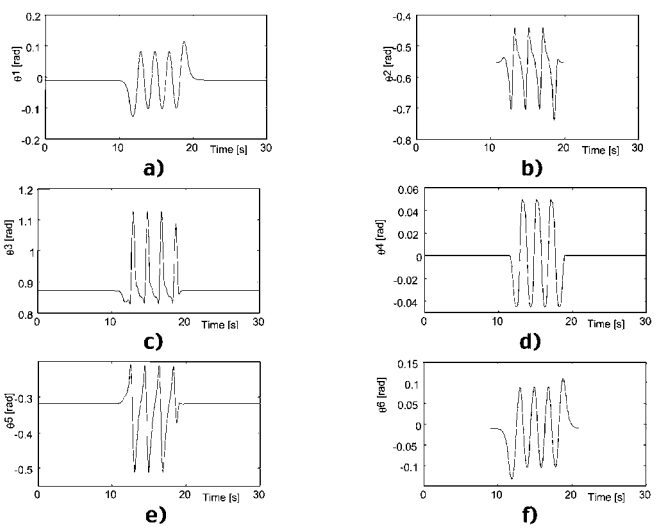


Fig. 12. Joint angles [rad] versus time [sec] as generated by the pattern planning algorithm for a four step turn left motion of WABIAN-RIV: (a) θ_1; (b) θ_2; (c) θ_3; (d) θ_4; (e) θ_5; (f) θ_6.

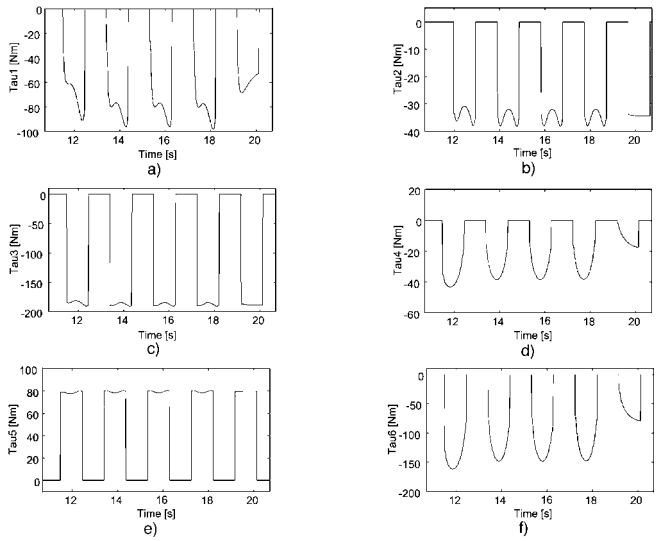


Fig. 13. Input torques [Nm] versus time [sec] as obtained from the numerical simulation for the leg motion by using the data in Figure 11: (a) τ_1; (b) τ_2; (c) τ_3; (d) τ_4; (e) τ_5; (f) τ_6.

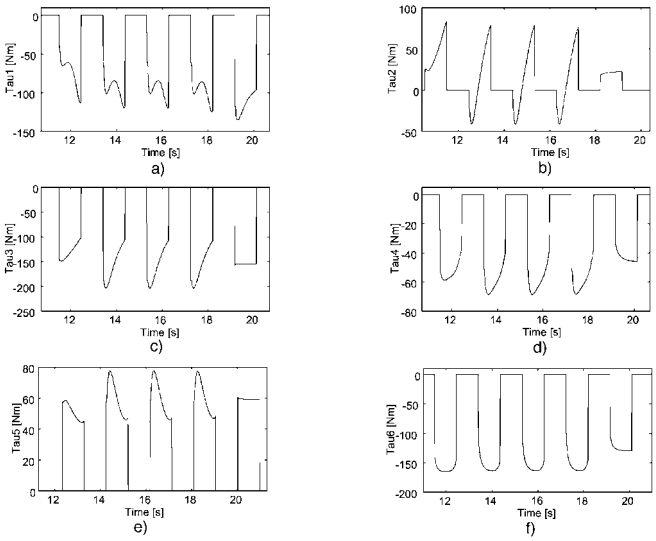


Fig. 14. Input torques [Nm] versus time [sec] as obtained from the numerical simulation for the leg motion by using the data in Figure 12: (a) τ_1; (b) τ_2; (c) τ_3; (d) τ_4; (e) τ_5; (f) τ_6.

a function of time as shown in Figures 15 and 16 for the same cases of the numerical simulations whose results are shown in Figures 13 and 14, respectively. Also for these cases the comparison of numerical and experimental results shows a good match between numerical and experimental results, both in maximum values and shapes of torque plots versus time. In particular, the maximum absolute difference can be evaluated as 5.5 Nm, and the maximum percentage difference is 5.9% for the case of a four steps right side motion as shown in Table III. The maximum absolute difference can be evaluated as 7.7 Nm, and the maximum percentage difference is 11.0% for the case of a four steps turn left motion as shown in Table IV.

The good match between numerical and experimental results can allow us to consider as validated the proposed formulation. Therefore, the proposed model of dynamics

https://doi.org/10.1017/S0263574703005393 Published online by Cambridge University Press

can be considered suitable as a design tool for the new leg prototype.

4.2 Input Torques for the New Leg Module

After experimental validation the proposed dynamics model has been used in order to determine the needed input torques for the new leg module. As for the case of a WABIAN-RIV, the kinematics and leg motion (position, velocity and acceleration of all the joints), mass and inertia distribution of the new leg prototype are needed as inputs for the proposed dynamics simulation. Nevertheless, mass and inertia distribution are unknowns in a design procedure, since they depend also on the mass and inertia of the motors. Therefore, a trial-error procedure has been carried out in order to consider in the dynamics simulation the masses and inertia parameters of the motors that can provide the required input torques for a given set of leg motions. As regards the leg motion, the pattern planning algorithm implemented for the WABIAN-RIV has been modified in a suitable way to consider the kinematic model of the new leg module. By using this modified pattern planning algorithm all the input angles as function of time can be computed.

The above-mentioned input data have been used for the evaluation of the needed torques in the new leg prototype by using Equations (2)–(4) as for example for the cases of a three step forward motion at a maximum velocity of 0.83 m/s, a three step right side motion at a maximum velocity of 0.1 m/s and a turn left motion. Results of the proposed numerical simulations have been the plots of the input torques τ_1, τ_2, τ_3, τ_4, τ_5, τ_6, τ_7 as a function of time that are shown in Figures 17, 18 and 19. The maximum values of the torques numerically computed are shown in Table V. These values and angular velocities for each joint given by the pattern planning algorithm have been used in order to size

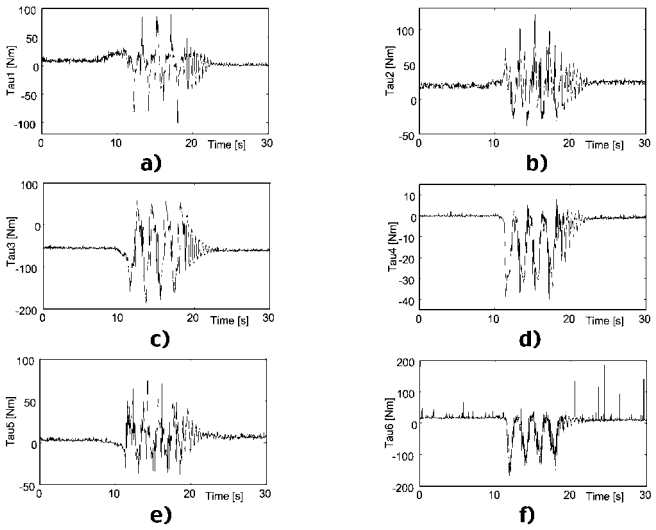


Fig. 15. Input torques [Nm] versus time [sec] measured experimentally for the leg motion by using the data in Figure 11: (a) τ_1; (b) τ_2; (c) τ_3; (d) τ_4; (e) τ_5; (f) τ_6.

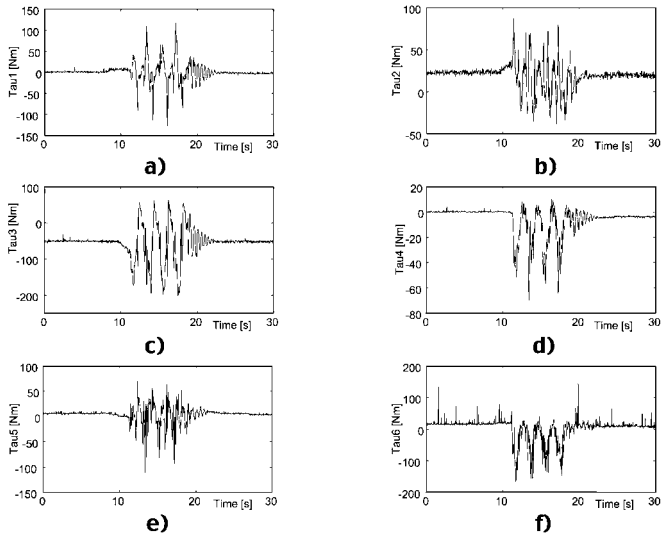


Fig. 16. Input torques [Nm] versus time [sec] measured experimentally for the leg motion by using the data in Figure 12: (a) τ_1; (b) τ_2; (c) τ_3; (d) τ_4; (e) τ_5; (f) τ_6.

Table III. Comparison of the maximum torques obtained from the numerical and experimental data reported in the plots of Figures 11 and 13, respectively.

	τ_{1max}[Nm]	τ_{2max}[Nm]	τ_{3max}[Nm]	τ_{4max}[Nm]	τ_{5max}[Nm]	τ_{6max}[Nm]
Numerical	− 98.3	− 38.2	− 191.0	− 43.1	80.6	− 161.5
Experimental	− 102.3	− 39.9	− 189.1	− 40.7	83.4	− 167.0
Absolute difference	− 3.9	− 1.7	1.9	2.4	− 2.8	− 5.5
Percentage difference	4.0%	4.3%	1.0%	5.9%	− 3.4%	− 3.3%

Table IV. Comparison of the maximum torques obtained from the numerical and experimental data reported in the plots of Figures 12 and 14, respectively.

	τ_{1max}[Nm]	τ_{2max}[Nm]	τ_{3max}[Nm]	τ_{4max}[Nm]	τ_{5max}[Nm]	τ_{6max}[Nm]
Numerical	− 135.5	− 41.4	− 204.0	− 68.6	77.7	− 164.6
Experimental	− 128.5	− 38.3	− 201.3	− 70.0	70.0	− 166.8
Absolute difference	7.0	3.1	2.7	− 1.4	7.7	2.2
Percentage difference	5.4%	8.1%	1.3%	− 2.0%	11.0%	− 1.3%

https://doi.org/10.1017/S0263574703005393 Published online by Cambridge University Press

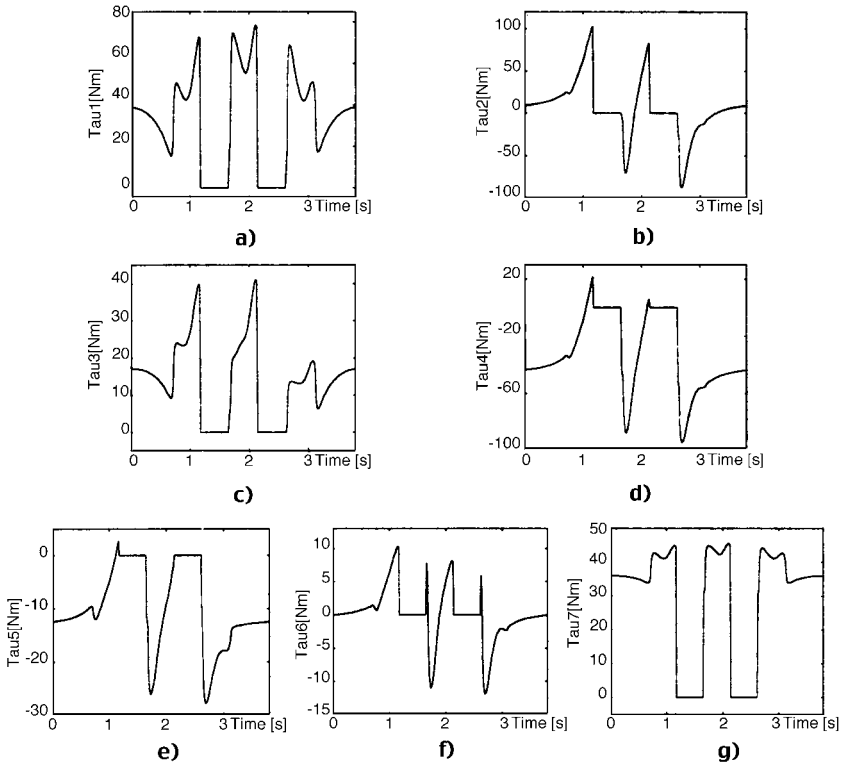


Fig. 17. Input torques [Nm] versus time [sec] given by the numerical simulation of the new leg prototype in the case of a three steps forward motion at a maximum velocity of 0.83 m/s: (a) τ_1; (b) τ_2; (c) τ_3; (d) τ_4; (e) τ_5; (f) τ_6; (g) τ_7.

all the motors and transmission ratios, as shown in Table VI.

It is worth noting that in the choice of actuators and transmissions only commercially available components have been considered and that dimensions and weight of each component have been taken into account. The lack in the market of an actuator that is able to provide the needed torque is a serious constraint for the designer of humanoid robots. In fact, in this field the choice of an over dimensioned actuator, which is bigger and heavier, has to be avoided since an over-dimensioned actuator can exceed the dimensional constraints given by the anthropomorphic design, or at least reduce significantly the overall performances. On the other side, manufacturers usually provide a serial production of actuators. Each type of product available in the market usually has a big difference in terms of nominal/maximum torque and dimensions. In reference [25], for example, the DC brushless motor series is available in 10 different models having nominal power of 1.2, 10, 15, 20, 50, 80, 120, 150, 250, 400 watts, respectively. The same motors have a maximum size of 21, 44.5, 49.5, 60, 62.7, 67.7, 70, 111.2, 144, 177.3 mm, respectively. Therefore, the

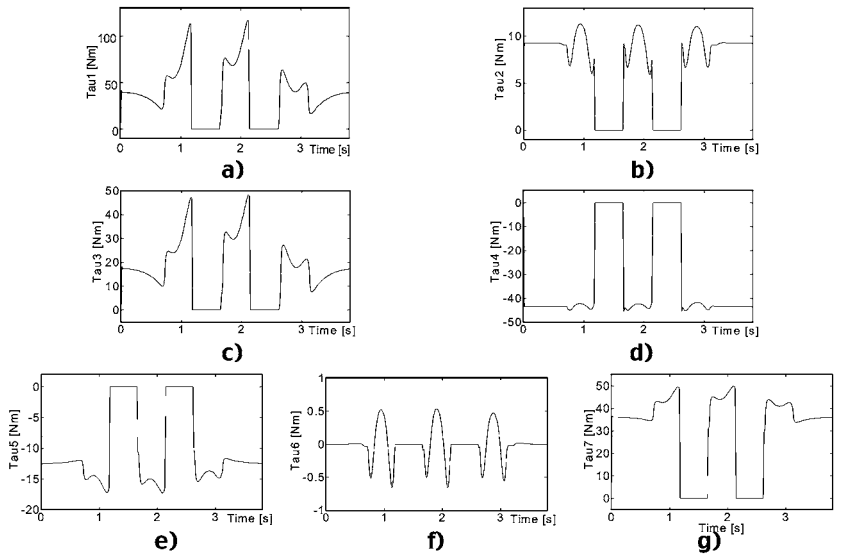


Fig. 18. Input torques [Nm] versus time [sec] given by the numerical simulation of the new leg prototype in the case of a three steps right side motion at a maximum velocity of 0.1 m/s: (a) τ_1; (b) τ_2; (c) τ_3; (d) τ_4; (e) τ_5; (f) τ_6; (g) τ_7.

https://doi.org/10.1017/S0263574703005393 Published online by Cambridge University Press

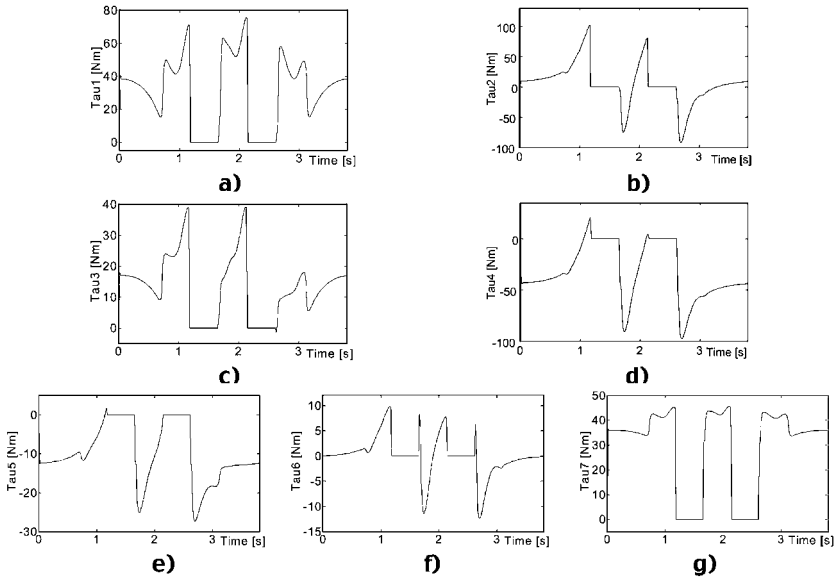


Fig. 19. Input torques [Nm] versus time [sec] given by the numerical simulation of the new leg prototype in the case of a three steps turn left motion: (a) τ_1; (b) τ_2; (c) τ_3; (d) τ_4; (e) τ_5; (f) τ_6; (g) τ_7.

Table V. Maximum torques from the proposed numerical simulation for the new 7-dofs leg.

Motion	Simulation Results	Joint 1	Joint 2	Joint 3	Joint 4	Joint 5	Joint 6	Joint 7
3 steps forward	τ_{max} [Nm]	78.6	102.9	41.1	− 94.3	− 27.9	− 12.0	45.5
3 steps right side	τ_{max} [Nm]	116.7	11.3	48.4	− 45.5	− 17.2	− 0.7	49.9
3 steps turn left	τ_{max} [Nm]	75.8	102.4	39.2	− 97.4	− 27.3	− 12.4	45.6

Table VI. Maximum torques and total transmission ratios for the chosen components.

Chosen actuator τ_{max} [Nm]	0.389	0.389	0.050	0.389	0.050	0.389	0.389
Chosen transmission ratio	381.8	275	1000	320	1000	275	392.7
Maximum torque available on the input shaft [Nm]	148.5	107.0	50.0	124.5	50.0	107.0	152.8

difference between a product and another in terms of maximum size and nominal power can be more then 50%. Also the available reduction gears give a further constraint since they are available with a limited number of reduction ratios and dimensions. For example, the Maxon planetary gearhead GP26 is available with reductions of 13/3, 169/9, 299/9, 2197/27, 3887/27, 598/3, respectively, and only three sizes are available: 28.7, 36.7 and 44.7 mm.[25] The above-mentioned considerations sometimes force the designer to overload the actuators during short term operation by using data on this type of operation provided by the manufacturer and/or previous experimental tests.

5. CONCLUSIONS

In this paper, a numerical dynamics simulation by means of Newton-Euler equations has been formulated for the walking of the leg module of a WABIAN-RIV humanoid robot. Experimental tests have been carried out and a good match between numerical and experimental results has validated the proposed formulation. The validated formulation has been used in order to simulate the dynamics of a new leg module having 7-dofs. By using the results of this simulation the actuator sizes for the new leg prototype have been properly chosen.

ACKNOWLEDGEMENTS

The first author is thankful to the Italian Ministry MIUR for the research project RIME in the program PRIN01 and the Italian National Research Council CNR for the grant 203.21.04, that have permitted him to spend periods of study in the years 2002 and 2003 at the Humanoid Robotics Institute, Waseda University, Tokyo.

References

1. T. Fukuda, R. Michelini, V. Potkonjak, S. Tzafestas, K. Valavanis and M. Vukobratovic, "How far away is artificial man?", *IEEE Robotics & Automation Magazine* **7**(1), 66–73 (2001).
2. M.E. Rosheim, *Robot evolution. The development of anthrobotics*. John Wiley & Sons (1994).
3. P. Artrit, N. Tsagarakis, G.A. Medrano-Cerda and D.G. Caldwell, "Bio-mimetic pneumatic humanoid robot-biped locomotion", *Proceedings of 3rd International Conference on Climbing and Walking Robots and the Support Technologies for Mobile Machines*, M. Armada and P.G. De Santos (Editors) (2000), pp. 221–230.

https://doi.org/10.1017/S0263574703005393 Published online by Cambridge University Press

4. G. Carbone, M. Ceccarelli, A. Takanishi and H.O. Lim, "A study of feasibility for a low-cost humanoid robot", *Proceedings of IEEE-RAS International Conference on Humanoid Robots HUMANOIDS 2001*, Tokyo (2001), pp. 351–358.
5. B. Espiau and BIP team, "BIP: A joint project for the development of an anthropomorphic biped robot", *Proceedings of IEEE International Conference on Advanced Robotics*, Monterey (1997), pp. 267–272.
6. Y.F. Zheng and J. Shen, "Gait synthesis for the SD-2 biped robot to climb sloping surface", *IEEE Transactions on Robotics and Automation* (6), 86–96 (1990).
7. A. Nishi, "A biped walking robot capable of moving on a vertical wall", *Mechatronics* (2), 543–554 (1992).
8. G. Figliolini and M. Ceccarelli, "Mechanical design of an anthropomorphic electropneumatic walking robot", *Proceedings of the 11th CISM-IFToMM Symposium on Theory and Practice of Robots and Manipulators RoManSy* 11 (Springer-Verlag, Wien, 1996), pp. 189–196.
9. M. Ceccarelli and G. Figliolini, "Proyecto de un mecanismo para un robot bipedo", *III Congreso Iberoamericano de Ingegneria Mecanica, CD Proceedings*, La Habana, paper 3-286 (1997).
10. G. Figliolini and M. Ceccarelli, "Walking programming for an electropneumatic biped robot", *Mechatronics: An International Journal* (9), 941–964 (1999).
11. G. Figliolini, M. Ceccarelli and V. Di Cocco, "Binary pneumatic actuators for a leg mechanism of walking robot", *3rd International Conference on Climbing and Walking Robots*, Madrid, (2000), pp. 575–582.
12. G. Figliolini and M. Ceccarelli, "Gait analysis of EP-WAR2 biped robot for walking and climbing stairs", *Proceedings of 4th International Conference on Climbing and Walking Robots ClaWar2001* (Professional Engineering Publications, London, 2001), pp. 827–834.
13. M. Vukobratovic, B. Borovac, D. Surla and D. Stokic, "Biped locomotion, dynamics, stability, control and application" (Springer, Berlin, 1990).
14. A.A. Grishin, A.M. Formal'sky, A.V. Lensky and S.V. Zhitomirsky, "Dynamic walking of two biped vehicle", *Proceedings of 9th World Congress on the Theory of Machines and Mechanisms*, Milano (1995), pp. 2308–2312.
15. S. Kawaji, K. Sawada and K. Ogasawara, "Dynamic walking of biped locomotion robot using kicking motion", *Proceedings of the International Conference on Advanced Robotics*, Tokyo (1993), 501–506.
16. C.L. Shin, "The dynamics and control of a biped walking robot with seven degrees of freedom", *ASME Journal of Dynamic Systems, Measurement, and Control* (118), 683–690 (1996).
17. P. Gorce and M. Guihard, "On dynamic control of pneumatic bipeds", *Journal of Robotic Systems* (15), 421–433 (1998).
18. H.O. Lim, A. Ishii and A. Takanishi, "Emotion-based walking of a biped humanoid robot", *13th CISM-IFToMM Symposium on Theory and Practice of Robots and Manipulators Ro.Man.Sy 2000* (Springer-Verlag, Wien, 2000), pp. 295–306.
19. S. Hashimoto, S. Narita, H. Kasahara, A. Takanishi, S. Sugano, K. Shirai and T. Kobayashi, "Humanoid robots in Waseda University – Hadaly-2 and WABIAN", *Humanoid and Human Friendly Robotics IARP'98*, paper I-2 (1998).
20. Waseda University homepage, http://www.humanoid.waseda.ac.jp.
21. B. Dasgupta and P. Choudhury, "A general strategy based on the Newton-Euler approach for the dynamic formulation of parallel manipulators", *Mechanism and Machine Theory* **34**(6), 801–824 (1999).
22. J.J. Craig, *Introduction to robotics* (Addison-Wesley Publishing Co., Reading, 1986).
23. H.O. Lim, S.A. Setiawan and A. Takanishi, "Balance and impedance control for biped humanoid robot locomotion", *Proceedings of IEEE-RSJ International Conference on Intelligent Robots and Systems IROS 2001*, Maui (2001), pp. 494–499.
24. H. Naoki, "Online whole body motion pattern generation for a bipedal humanoid robot", Master Thesis, Waseda University, Tokyo, 2001 (in Japanese).
25. Maxon Motor AG, "Maxon 2001", *Product Catalogue* (Sachseln, 2001).

https://doi.org/10.1017/S0263574703005393 Published online by Cambridge University Press